Analysis of Rain Clutter Detections in Commercial 77 GHz Automotive Radar

Rossiza Gourova*, Oleg Krasnov† and Alexander Yarovoy‡
Microwave Sensing, Signals and Systems (MS3) group
Delft University of Technology
Mekelweg 4, 2628 CD, Delft, the Netherlands
*r.gourova@tudelft.nl, †o.a.krasnov@tudelft.nl, ‡a.yarovoy@tudelft.nl

***Abstract*—This paper investigates the impact of rain on performance of 77 GHz radar. The experiments performed in a rain-fog tunnel show radar detections, attributed to rain, at very short ranges for high rain intensities. The theoretical analysis of rain clutter demonstrates a possibility of rain detection by a radar with narrow beam at short ranges.**

I. Introduction

Rain causes multiple effects which decrease the radar's performance, such as attenuation of the signal and increase of the non stationary clutter. The attenuation of the signal has two reasons - the wetness of the bumper or other car dielectric surface that operates as radar radome, and the absorptions in and scattering on rain drops within the propagation path. The interaction of the radar and the dry bumper was analysed in [1] and the attenuation of the bumper was studied for the purpose of optimizing the dry bumper construction to radar signals in [2], [3]. Not much attention, however, is given on how water on the bumper influences radar operation. Studies that focus on this problem are [4] and a more recent work [5], focused on a general description of the scattering from a wet surface.

Due to the electromagnetic wave attenuation in rain, the range of the radar is decreased which has impact on the targets detectability [6]. Various models exist for the estimation of the attenuation caused by rain. For example, in [7] different rain models are compared to experimental data, obtained with a 77 GHz radar in a climatic wind tunnel. One of the used models follows the ITU-R P.838-3 recommendations [8]. The attenuation of communication links at 75 and 85 GHz was studied using real rain measurements in [9]. The results presented there, however, are relevant to communication links, where the propagation distances far exceed the maximum distance of 250 m for long range automotive radar.

Usually, the literature on rain effect on radar assumes access to low level data and knowledge on the processing of this data. The state-of-the-art radars used in the car industry, however, are based on company know-how where little or no information is provided for the internal functioning of the device. To evaluate the radar performance in rain and fog from the point of view of the driver support system, which has no access to the lower level data, an experimental campaign was conducted. In this paper some observations from the measurement campaign are presented and a theoretical analysis is performed with the aim to explain the findings.

The paper is organized as follows: Section II introduces the automotive radar used, for the experiments set-up and the analysis. Section III discusses the rain attenuation and the theoretical background of rain reflectivity, and Section IV focuses on conclusions and future work.

II. Experiments

A. Experiments location and set-up

The tests at the weather tunnel of Cerema, a French research institution located in Clerment-Ferrand, were performed on 30th March 2016.

The weather tunnel has two sections - the first of 15 m and the second of 16 m. The second section of the tunnel is a green house which can be half opened on the top. A schematic of the tunnel and its characteristics can be found in [10].

The radar targets in the scene were 5 trihedrals. The wooden stands were painted beforehand in order to avoid them getting soaked in water. The targets were numbered and positioned as depicted in Fig.1 in the second half of the tunnel. In the Figure, the grey lines represent the wide and narrow beam of the radar. Opposite to the sensor, at the end of the second part of the tunnel, is situated a parked car. During the measurement the sensor and the measured targets had fixed positions.

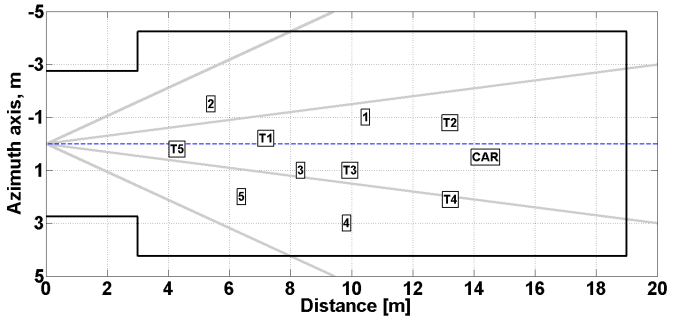

Fig. 1. Radar test set-up in weather tunnel. Targets - T1-T5: thrihedrals; 1: traffic sign; 2: triangular sign; 3&5: video signs; 4: mannequin

Measurements were taken in both foggy and rainy conditions. The analysis of the data taken in fog did not reveal influence of this event on the radar. Thus, the rest of the paper deals with the rain experiments. All experiments were conducted without a dielectric bumper in front of the radar,

and the attenuation effect of the dielectric bumper in both foggy and rainy conditions is not evaluated in this study. In the case when there is a radome, the attenuation is expected to increase due to the continuous water layer formed on the dielectric surface as a result of the fog or the rain.

The rain and the fog were artificially created and the information provided by Cerema to characterize the weather conditions was a record of the visibility during the measurements. The visibility was measured using transmissometers as described in ch.9 of [11]. For the foggy case, the visibility was decreased to 17-20 m. The relation of the visibility to the rainfall rate is [12]:

$$Vis \approx 9.3 I^{-0.67} \tag{1}$$

where the visibility, Vis, is in km and the rain rate I is in mm/h. Using the above formula, the rain rate from the Cerema measurements can be calculated to be ≈24 mm/h for the moderate rain. For the heavy rain case it is not possible to calculate the rain rate as the visibility data is corrupted due to obstacles in front of the transmissometers.

B. Automotive 77 GHz radar - Continental ARS300

The radar used for the experiments is Continental ARS300. This is a long range radar especially designed for the automotive industry and used in commercial vehicles. Some of its main parameters are shown in Tab.I. Further information about the radar is available in [13]. The gain of the radar can be approximately calculated using the provided beamwidth for the wide G^{wb} and narrow beam G^{nb} as follows [14]:

$$G \approx \epsilon \frac{4\pi}{\theta_a \theta_e} \tag{2}$$

where , θ_a and θ_e are respectively the azimuth and elevation $-3\,dB$ beamwidth of the radar and ϵ is the efficiency of the antenna. For the purpose of this paper the efficiency is assumed $\epsilon = 0.9$. For the two beams of the radar the calculated gains are: $G^{nb} = 39.36$ dB and $G^{wb} = 33.34$ dB

By measurements involving a network and a spectrum analyzer, the bandwidth of the device was determined to be 75 MHz for the maximal range of the beams. Because the radar is a commercial product with quite limited technical details available in documentation, it has limited controls. One of them is the ability to change the range which also affects the bandwidth - as the range decreases the bandwidth increases. The polarization was determined to be horizontal.

The radar has two modes - target list and object list. In object mode, only the tracked objects are provided, whereas in target mode all detections are delivered. In target mode, which was used for the presented experiments, twelve parameters are delivered per target, the most important are range, azimuth angle, velocity and RCS. More information about all the parameters and the CAN messages can be found in [15].

C. Observations

The data was continuously recorded with PC USB to CAN interface, during the changing weather conditions. The logged data was then converted to Matlab structure array. Further analysis were conducted in Matlab.

TABLE I
CONTINENTAL ARS300 CHARACTERISTICS

Transmit power P_t		<10mW
Central frequency f_c		77.5 GHz
Transmitted waveform		Chirped radar modulation
Elevation beamwidth θ_e		4.3°
Azimuth beamwith	Wide beam θ_a^{wb}	4°
	Narrow beam θ_a^{nb}	1°
Range / Field of View	Wide beam	0.25...60 m / $-28° ... + 28°$
	Narrow beam	0.25...200 m / $-8.5° ... + 8.5°$
Cycle time		≈66 ms for close and far measurements
Range resolution ΔR		2m

* The presented information is collected from [13]

A histogram map of the detections for 8760 cycles before and during the rain event are presented in Fig.2. The colour scale represents the number of detections per spatial bin. It is important to note that the colour scale is restricted and it does not represent the maximum number of detections on the figures. This restriction is made in order to make all detections more visible. The data analysis shows that rain detections took place mostly in the first 2-3m in front of the radar and are only visible within the far beam mode. The narrow and the wide beams are assumed to emit the same energy, but for the narrow beam the gain is increased. Even though the narrow beam has higher gain and, thus, higher received power for point targets, the reflections originating from rain are possibly smaller due to the decreased scattering volume.

The reflections with RCS below 0 dBm^2 in the first 3 m were further analysed and the histogram of their respective RCS and velocity is shown in Fig.3. The targets on the scene were static, but the detections attributed to the rain drops have non zero velocity. This fact, the low measured RCS and their characterization from the radar as real targets confirms that the detections are caused by rain.

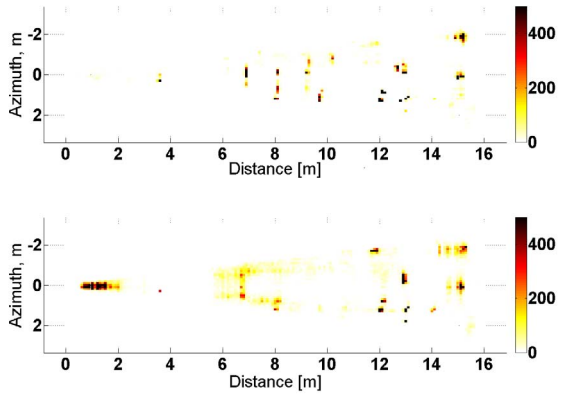

Fig. 2. Histogram of detections observed for 8760 cycles with narrow beam before (top) and during (bottom) rain event

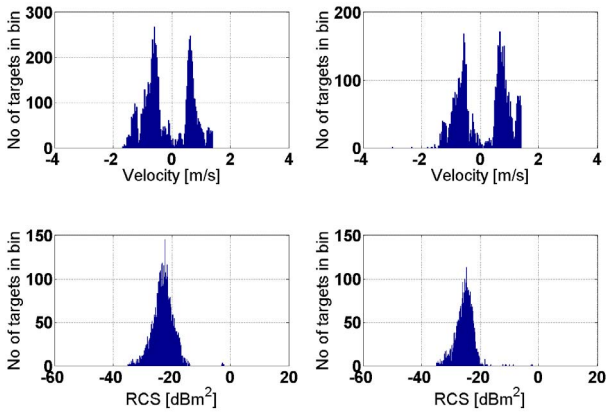

Fig. 3. Histograms for targets of RCS$\leq$0 and range$\leq$3 m observed with narrow beam. Top: Velocity histogram with bin size 0.03 m/s - heavy rain (left), moderate rain of $\approx 25\,mm/h$ (right); Bottom: RCS histogram with bin size 0.1 dBm^2 - heavy rain (left), moderate rain (right)

III. Rain impact on 77 GHz radar signal

A theoretical analysis of the behaviour of the rain at 77 GHz was conducted in order to explain the rain observations made during the Cerema campaign.

A. Attenuation

The attenuation was not considered as it has little impact at short distances. ITU recommendation P.838 [8], specifies how the specific attenuation in rain can be calculated. Using the formula specified there, the specific attenuation for 76.5 GHz at different rain rates ranges from 0.0016 dB/m for 1 mm/h to 0.032 dB/m for 100 mm/h. This implies that at close distances ($\leq$30 m), the attenuation caused by rain does not have a large effect on the radar signal, hence it is not relevant for this study.

B. Rain backscattering

The received by the radar power from rain is calculated as:

$$P_r = \frac{P_t G^2 \lambda^2}{(4\pi)^3 R^4} \sigma_{rb} = C_r \sigma_{rb} \tag{3}$$

where σ_{rb} is the rain radar cross section (RCS), C_r is the radar constant, P_t is the transmitted power, and $\lambda = c/f_c$ is the wavelength, f_c is the central frequency.

Figure 4 presents the radar constant for the wide and narrow beam of the Continental ARS300, under the assumption that the transmitted power remains the same for both beams of the radar. Taking into account the calculated in Section II-B gains, the larger gain of the narrow beam contributes to a larger radar constant by 12 dB for the two way propagation.

From the dependence of the beam volume on the range it is known that the received backscattered power from rain will change with R^2 instead of R^4 as for the target echo. This contributes to the decrease of the maximum range of the detectability as discussed in [4] and [6].

The rain backscattering can be expressed as:

$$\sigma_{rb} = \eta V \tag{4}$$

where η is the rain reflectivity and V is the resolution cell volume which can be calculated as follows:

$$V = \pi R^2 \tan\frac{\theta_a}{2} \tan\frac{\theta_e}{2} \Delta R \tag{5}$$

where R is the range at which the volume is calculated and $\Delta R = c/2B$ is the range resolution, c is the speed of light and B the bandwidth. The resolution cell volume for the first 5 m of the two beams of the Continental radar is presented in Fig.4. The received power from the wide beam is expected to be 6 dBm lower than that of the narrow beam.

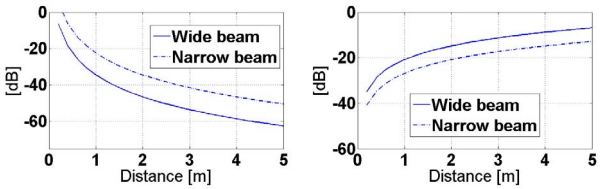

Fig. 4. Radar constant (left) and Resolution cell volume (right)

The rain reflectivity can be expressed as the summation of the RCS of all raindrops per unit volume [16]:

$$\eta = \int_0^\infty \sigma(\lambda, D) N_D(D) dD \tag{6}$$

where $\sigma(\lambda, D)$ is the rain backscattering from a single drop with diameter D, and $N_D(D)$ is the raindrop distribution. The rain backscattering of one drop with assumed spherical shape can be calculated according to Mie scattering [16]. The code from [17] was used for the Matlab execution of the Mie scattering. For $\pi D/\lambda \ll 1$, the Mie scattering can be simplified by using Rayleigh's approximation. At 77 GHz, however, this approximation is only valid for $D \leq$1 mm as shown in Fig.5. This mismatch between the Rayleigh approximation and the Mie scattering causes large difference in the calculation of the reflectivity as shown in Fig.5.

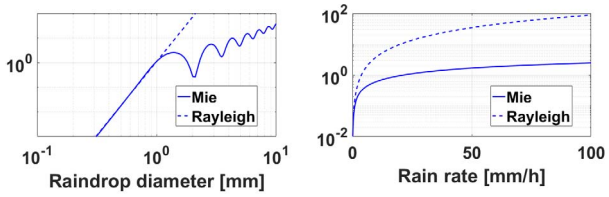

Fig. 5. Rain backscattering and reflectivity for 76.5 GHz for temperature $T = 10°$ C. Rayleigh and Mie backscattering coefficients (left) and Rain reflectivity at different rain rates (right)

The Marshall-Palmers drop size distribution (DSD) [18]

$$N_D(D) = N_0 \exp(-\Lambda D) \qquad [cm^{-4}] \tag{7}$$

where $N_0 = 0.08\,\mathrm{cm}^{-4}$, $\Lambda = 41 I^{-0.21}\,\mathrm{cm}^{-1}$ and D is the drop size diameter in cm, with maximum diameter D_{max}. Finally, the rain RCS is calculated for the first 5 m using equation (4). The results are shown in Fig. 6 (top). The theoretically calculated RCS values fit well with the observed values presented in Fig.3. The RCS of the rain for wide beam

is higher, but the received power is lower. This means that in case the same threshold is used for both beams, the returns from the narrow beam are more likely to be detected than those of the wide beam. The received power from both beams is presented in Fig. 6 (bottom). An arbitrary threshold is taken at -50 dBm level to demonstrate the lower return power in wider beam which hardly passes the threshold even for very strong rain and only at very close distance to the radar.

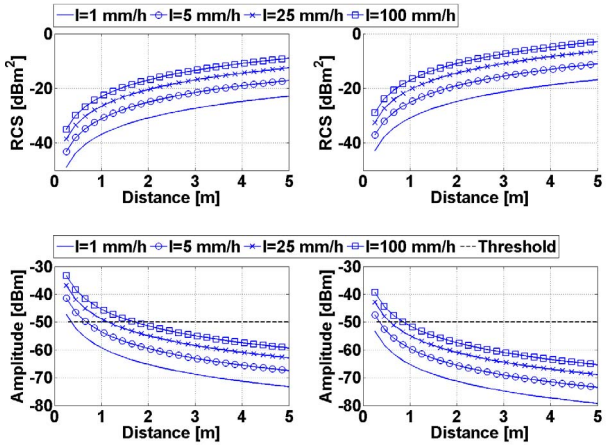

Fig. 6. Rain RCS and received power for different rain rates. Top: Rain RCS for narrow beam (left) and Rain RCS for wide beam (right); Bottom: Received power for narrow beam (left) and Received power for wide beam (right)

The formulas described in this section were used to calculate the theoretical rain RCS for the measured ranges. The distributions were then fitted to the measured RCS using the rain rate which resulted in the closest mean of the two distributions. The rain rate achieved in this manner is 22.5 mm/h for the moderate rain and 58.5 mm/h for the heavy rain. For the moderate rain this is a good fit to the rain rate calculated using equation (1). The resulting distributions are presented in Fig. 7.

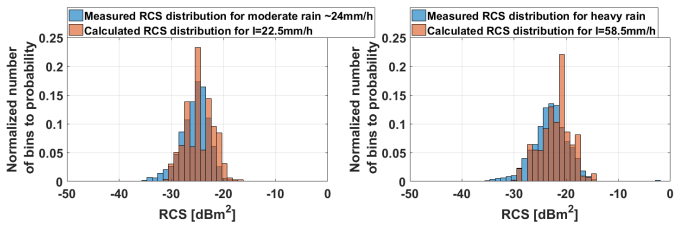

Fig. 7. Normalized histogram of RCS for targets at range$\leq$3 m observed with narrow beam. Moderate rain (left) and heavy rain (right)). Bin size is 1 dBm^2.

IV. Conclusion and Future work

The influence of rain on commercial radar performance is presented. The measurements and the analysis were made for an automotive radar where broad and pencil beams were used. The experimental data demonstrate the detectability of strong rain with narrow beam. A theoretical analysis of the rain backscattering for two different beamwidths at close ranges was made as an attempt to explain the observed radar detections. Good agreement between the theoretical analysis and the experimental data was observed.

Of particular interest as a future study is to use the characteristics of this rain returns as parameters for the detection of rain events. In this sense, the influence of the rain on the target detection should be further investigated. The fluctuation of the RCS and the possible increase of positioning inaccuracies of the targets are of interest as target characteristics of the rain.

Acknowledgements

This work is supported by NWO Domain TTW, the Netherlands, under the project S4DRIVE - TTW # 13434.

The authors would like to thank ing. T. Dalhuisen, ir. J. Domhof and ing. E. Goossens for their support before and during the experiments. The authors are gratefull to Steery for the invitation to take part in the measurement campaign.

References

[1] R. Schnabel, D. Mittelstrab, T. Binzer, C. Waldschmidt, and R. Weigel, "Reflection, refraction, and self-jamming," *Microwave Magazine, IEEE*, vol. 13, no. 3, pp. 107–117, 2012.

[2] F. Fitzek and R. H. Rasshofer, "Automotive radome design-reflection reduction of stratified media," *Antennas and Wireless Propagation Letters, IEEE*, vol. 8, pp. 1076–1079, 2009.

[3] F. Pfeiffer and E. M. Biebl, "Inductive compensation of high-permittivity coatings on automobile long-range radar radomes," *Microwave Theory and Techniques, IEEE Transactions on*, vol. 57, no. 11, pp. 2627–2632, 2009.

[4] A. Arage Hassen, "Indicators for the signal degradation and optimization of automotive radar sensors under adverse weather conditions," Ph.D. dissertation, TU Darmstadt, 2007.

[5] N. Chen, "Millimetre wave propagation and scattering phenomena for automotive radar," Master's thesis, Delft University of Technology, The Netherlands, 2016.

[6] J. Huang, S. Jiang, and X. Lu, "Rain backscattering properties and effects on the radar performance at mm wave band," *International Journal of Infrared and Millimeter Waves*, vol. 22, no. 6, pp. 917–922, 2001.

[7] U. J. Lewark, T. Mahler, J. Antes, F. Boes, A. Tessmann, R. Henneberger, I. Kallfass, and T. Zwick, "Experimental validation of heavy rain attenuation in e-band based on climate wind tunnel measurements at 77 ghz," *CEAS Space Journal*, vol. 7, no. 4, pp. 475–481, 2015.

[8] ITU, "Specific attenuation model for rain for use in prediction methods," *Recommendation ITU-R P.838-3*, 2005.

[9] J. M. García-Rubia, J. M. Riera, P. Garcia-del Pino, and A. Benarroch, "Attenuation measurements and propagation modeling in the w-band," *IEEE Transactions on Antennas and Propagation*, vol. 61, no. 4, pp. 1860–1867, 2013.

[10] Cerema, "Fog & rain r&d platform," http://www.infra-transports-materiaux.cerema.fr/IMG/pdf/04_Rain_Fog_lolo.pdf, online; accessed 03 October 2016.

[11] M. Jarraud, "Guide to meteorological instruments and methods of observation (wmo-no. 8)," *World Meteorological Organisation: Geneva, Switzerland*, 2008.

[12] D. Atlas, "Optical extinction by rainfall," *Journal of Meteorology*, vol. 10, no. 6, pp. 486–488, 1953.

[13] "Technical description of the radar system ars300 industrial," Continental Temic, rev. 2.3; Not available online.

[14] I. S. Merrill *et al.*, "Introduction to radar systems," *Mc Grow-Hill*, 1981.

[15] "Standardized ars interface; technical documentation," http://www.conti-online.com/www/download/industrial_sensors_de_de/themes/download/1can_ars308_technical_docu_2012_05_31.pdf, Continental Temic, v1.13; Online; accessed 23 January 2017.

[16] G. P. Kulemin, *Millimeter-wave radar targets and clutter*. Artech House, 2003.

[17] C. Mätzler, "Matlab functions for mie scattering and absorption," *IAP Res. Rep*, pp. 1–18, 2002.

[18] J. S. Marshall and W. M. K. Palmer, "The distribution of raindrops with size," *Journal of meteorology*, vol. 5, no. 4, pp. 165–166, 1948.